ELECTROWEAK PHYSICS RESULTS FROM THE SLD

Frank E. Taylor*
Laboratory for Nuclear Science
Massachusetts Institute of Technology
Cambridge, MA 02139

Representing the SLD Collaboration

ABSTRACT

Data taken by the SLD Collaboration at the Stanford Linear Collider (SLC) on $e^+e^- \rightarrow Z^0$, obtained with a polarized electron beam, have enabled many incisive tests of the electroweak sector of the Standard Model to be performed. We discuss our recent determinations of $\sin^2\theta_W$, derived from the total cross-section asymmetry, and the quark final state asymmetries, A_s, A_c, A_b, and branching ratios, R_c and R_b. Aspects of the precision tests of the standard electroweak theory, involving radiative corrections, are described. Limits on the mass of the Higgs particle are given.

* Work supported in part by the Department of Energy.

1 Introduction

The theoretical description of electron-positron annihilation into the Z^0 vector boson is rich with experimentally testable predictions. Since the first data taken at LEP and SLC in 1990, experimental tests have been made of the Standard Model (SM) with ever increasing statistical and systematic precision. For some time, the data have been of sufficient quality to probe the radiative corrections related to the top quark and Higgs particle. To date, no experimental test of the SM has shown a persistent and confirmed deviation from theory. Rather than spectacular anomalies discovered, the experimental program at LEP-I and SLC is characterized as one of ever increasing refinement and verification of theory. At this time, the Z^0 pole data in conjunction with measurements at the FNAL collider of the W^+ boson and top quark masses are beginning to approach the untested Higgs sector of the theory.

The SLD-SLC facility[1] brings a number of unique features to the exploration of the SM at the Z^0 pole. The SLC produces Z^0s with polarized electrons colliding with unpolarized positrons in an exquisitely small intersection region that is roughly $1.6\ \mu m^2$ (700 μm) transverse (longitudinal) to the beam. The electron polarization provided by the SLC allows a quite precise measurement of $\sin^2\theta_W$ to be made with a statistical "boost" proportional to $|P_e|^2/A_e^2$, where P_e is the electron polarization and A_e is the axial coupling of the electron to the Z^0, by using the total cross section left-right asymmetry, A_{LR}. Tests of the SM can be performed on measurements of the properties of the final state, such as a study of the forward-backward left-right cross section asymmetry for b-quark final states. The SLD is equipped with a pixel vertex detector, based on the CCD technology, which is used to identify b- and c-quark final states and a Cherenkov ring imaging detector (CRID) for particle ID. The vertex detector has been recently upgraded, permitting better vertex resolution and coverage.[2]

Table 1 is a summary of the data taken at the SLD. Noteworthy is the outstanding accelerator operation during 1997-98, when the SLC delivered up to 20K polarized Z^0 events in a week. The total number of polarized Z^0 events is 560K with an "event-weighted" polarization of ~ 72%.

Table 1: History of SLD data taking.

Year	Purpose	Events	e^- Polarization
1992	physics	10K	22%
1993	physics	50K	63%
1994-5	physics	100K	77%
1996	physics & VXD3 commissioning	50K	77%
1997-8	physics	350K	73%

2 Basics of the Standard Model

For leptons at lowest order, the $SU(2)_L$ X U(1) standard model of Glashow-Weinberg-Salam[3] has the following Feynman rules for the neutral current (NC) and charged current (CC) fermion-gauge boson interactions, written in terms of the members of the first generation:

(a) $\gamma - e^+ e^-$ interactions (NC_γ):

$$-iQ_e \bar{e}\,\gamma_\lambda e, \qquad (1a)$$

(b) $Z^0 - f\bar{f}$ (f = e, ν) interactions (NC_Z):

$$\frac{-i}{\sqrt{2}}\left(\frac{G_F M_Z^2}{\sqrt{2}}\right)^{1/2} \bar{f}\gamma_\lambda(g_{V_f} - g_{A_f}\gamma_5)f, \tag{1b}$$

(c) $W^{\pm}$ – eν interactions (CC):

$$-i\left(\frac{G_F M_w^2}{\sqrt{2}}\right)^{1/2} \bar{\nu}\gamma_\lambda(1-\gamma_s)\,e, \tag{1c}$$

where G_F is the Fermi coupling constant, M_z the Z-boson mass, and g_v, g_A are NC vector and axial vector coupling constants, respectively. The two NC interactions, involving the exchange of γ or Z, are characterized by coupling strengths e and g', respectively, whereas the charged current (exchange of $W^{\pm}$) has a coupling strength $g \sim \sqrt{G_F}\, M_W$. The coupling constants involving the exchange of massive vector bosons ($W^{\pm}$ and Z^0) are related by the Weinberg mixing angle, θ_w, with $\tan\theta_w = g'/g$ and the electromagnetic neutral current is "unified" with the $W^{\pm}$ and Z interactions by $e = g'g/\sqrt{g'^2 + g^2}$. The NC interaction for a massive fermion pair coupled to the Z^0 has generally unequal right and left terms couplings g_{Re} and g_{Le}, respectively. The CC interaction is pure "V-A."

By the Higgs mechanism the vector boson masses, M_w and M_z, acquire mass of magnitude determined by the vacuum expectation value of the Higgs field, given by $\langle v \rangle = (\sqrt{2}G_F)^{-1/2} = 246$ GeV, and the coupling constants g and g'. The Fermi coupling constant, G_F, is the only "dimensioned number" in the theory. It is conventional to express the boson masses in terms of the experimentally determined constants α_{em}, $\sin^2\theta_w$ and G_μ, where α_{em} is the fine structure constant and is determined by the quantum hall effect and Thomson scattering at low energies, $\sin^2\theta_w$ is measured by a number of experiments, and $G_\mu = G_F$ by precision muon decay data. In this convention we have:

$$M_z^2 = \frac{\pi\alpha_{em}}{\sqrt{2}G_\mu \sin^2\theta_w \cos^2\theta_w \xi_Z}, \tag{2a}$$

$$M_w^2 = \frac{M_z^2}{2}\left(1 + \sqrt{1 - \frac{4\pi\pi_{em}}{\sqrt{2G_F}\xi_w M_z^2}}\right), \tag{2b}$$

where ζ_z and ζ_w are radiative correction terms, of order one, to be described later. The NC vector and axial vector couplings (or right- and left-handed couplings) for fermion f are given by:

$$g_{Vf} = (g_{Lf} + g_{Rf}) = I_{Lf}^3 - 2Q_f \sin^2\theta_w, \tag{3a}$$

$$g_{Af} = (g_{Lf} - g_{Rf}) = I_{Lf}^3, \tag{3b}$$

respectively, where I_{Lf}^3 is the third component of the weak isospin of fermion f, and Q_f is the corresponding electric charge. Since most of the precision electroweak data are at the Z pole, it is conventional to take $\sin^2\theta_w^{eff}$ to be the *effective value* at the pole,[4] thereby absorbing the radiation corrections in the gauge boson propagators. As such,

$$\sin^2\theta_w^{effective} = (1 - g_{Vf}/g_{Af})/4|Q_f|, \tag{4}$$

where g_{Vf} and g_{Af} are the *effective* vector and axial vector couplings of fermion f at the Z^0 pole.

Two important measurables at the Z^0-pole dependent on the coupling of $Z^0 \to f\bar{f}$ are the partial decay width given by

$$\Gamma_{f\bar{f}} = \frac{\sqrt{2}\, G_\mu\, M_Z^3}{12\pi} N_c \left(g_{Vf}^2 + g_{Af}^2\right) \zeta_{ff}, \tag{5a}$$

where N_c is the number of color degrees of freedom (N_c = 1 for leptons and 3 for quarks) and ζ_{ff} is a radiative correction term, of order one, and the coupling constant asymmetry, defined as:

$$A_f = \frac{g_{Lf}^2 - g_{Rf}^2}{g_{Lf}^2 + g_{Rf}^2} = \frac{2\, g_{Vf}\, g_{Af}}{g_{Vf}^2 + g_{Af}^2} = \frac{2\, g_{Vf} / g_{Af}}{1 + (g_{Vf}/g_{Af})^2} \quad . \tag{5b}$$

The coupling asymmetry for charged leptons is especially sensitive to the effective mixing angle, θ_w^{eff}. Table 2 shows the couplings, asymmetry, and sensitivity of the asymmetry to the effective mixing angle for the first generation quarks and leptons.

Table 2: First generation coupling constants and sensitivity of A_f to $\sin^2\theta_w^{eff}$ for $\sin^2\theta_w^{eff} = 0.23$.

f	I_{Lf}^3	Q_f	g_{Af}	G_{Vf}	G_{Lf}	G_{Rf}	A_f	$\frac{\delta A_f}{\delta \sin^2\theta_w}$
ν	1/2	0	1/2	1/2	1/2	0	1	0
e	-1/2	-1	-1/2	-0.04	-0.27	0.23	0.16	-7.9
u	1/2	2/3	1/2	0.19	0.35	-0.16	0.69	-3.5
d	-1/2	-1/3	-1/2	-0.35	-0.43	0.08	0.94	-0.6

Equations 1, 2, and 3, with radiative corrections, form the basis of precision tests of the electroweak sector of the SM. Equations 4, 5 and Table 2 furnish the tools and predictions of the SM. Note that the charged lepton couplings (e, μ, τ) are dominated by the axial term and have the greatest sensitivity for the determination of $\sin^2\theta_w$ and that the down quark couplings (d, s, b) are similar, but opposite sign, to the neutrino couplings and have a small sensitivity to $\sin^2\theta_w$. As a consequence, the down-like quark couplings lead to their being strongly polarized left-handed in Z^0 decay.

Some of the questions we have addressed to the data are:

- Is the Lorentz structure of the electroweak interaction described correctly by Eq. 1?
- Are the couplings for all generations and weak isospin states given by the theory isospin assignments and a *universal value* of $\sin^2\theta_w^{eff}$?
- Are the physical gauge boson masses related by Eq. 2?
- Do the higher order radiative corrections result in better consistency of the data?

2.1 Measurement of Weak Couplings

One of the fundamental tests of the SM afforded by data at the Z^0 pole is the check of the $SU(2)_L \times U(1)$ gauge group structure of the theory. It is of interest to see if Eqs. 3, 4, and 5 and the weak isospin and charge assignments of Table 2 are operative for all generations with the *same value* of $\sin^2\theta_w^{eff}$. This test is sensitive to putative Z^0s, indicating a new gauge group, or, as yet unobserved, new particles which could lead to non-universal radiative corrections for different generations.

In the context of the SM the differential cross section for $e^+e^- \to Z^0 \to f\bar{f}$ in the case, for example, of a left-handed electron producing a left-handed fermion in the final state, has the form

$$\sigma(\cos\theta) \sim g_{Le}^2\, g_{Lf}^2 \left(1 + \cos\theta\right)^2, \tag{8}$$

where θ is the angle of the final fermion with respect to the electron beam direction and g_{Le} and g_{Lf} are the left-handed electron and final fermion couplings to Z^0, respectively. Averaging over final fermion helicities for an electron beam with a polarization of P_e, the differential cross section has the form

$$\frac{d\sigma}{d\cos\theta} \sim (1-P_e A_e)\left(1+\cos\theta^2\right)+2\cos\theta\,(A_e - P_e)\,A_f \qquad (9)$$

Here, the electron and final fermion coupling asymmetry parameters A_e, A_f are given by Eq. 5b.

Figure 1 shows the differential cross section for the production of $(b\bar{b})$ for three electron beam polarization cases. Note that for left-handed incident electrons the b-quark tends to go in the forward hemisphere. This large production asymmetry is exploited by the SLD in b-quark studies in tests of the SM through electroweak coupling asymmetries and b-quark flavor mixing.

The basis of the measured asymmetries at LEP and SLC is given by Eqs. 10 (a-d). At LEP the forward-backward asymmetry ($P_e = 0$), given by

$$A_{FB}^f = \frac{\sigma_F^f - \sigma_B^f}{\sigma_F^f + \sigma_B^f} = \frac{3}{4} A_e A_f, \qquad (10a)$$

is a measure of the product of coupling asymmetries A_e, A_f. The forward-backward asymmetry is exploited at LEP to obtain lepton and quark couplings.

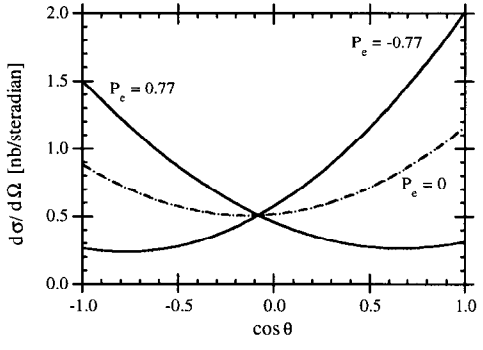

Figure 1: The differential cross section for $e^+e^- \rightarrow Z^0 \rightarrow b\bar{b}$ is shown for $P_e = \pm 0.77$, corresponding to polarized electron beams at SLC and $P_e = 0$, the operating condition for LEP.

The left-right total cross section asymmetry, exploited by the SLD Collaboration,[5] is given by

$$A_{LR} = \frac{\sigma_L - \sigma_R}{\sigma_L + \sigma_R} = |P_e| A_e, \qquad (10b)$$

where $\sigma_{L,R}$ are the $e^+e^- \rightarrow Z^0$ total cross sections for incident L, R electron polarizations and is the *centerpiece* of our precision electroweak tests at the SLC. Knowledge of the electron polarization $|P_e|$ allows the electron Z^0 coupling asymmetry, A_e, to be directly and quite accurately measured. The polarized forward-backward asymmetry, given by

$$A_{FB\_LR}^f = \frac{\left(\sigma_{FL}^f - \sigma_{BL}^f\right) - \left(\sigma_{FR}^f - \sigma_{BR}^f\right)}{\sigma_{FL}^f + \sigma_{BL}^f + \sigma_{FR}^f + \sigma_{BR}^f} = \frac{3}{4} |P_e| A_f, \qquad (10c)$$

allows a *direct determination* of the final state fermion coupling asymmetry parameters, A_f. This asymmetry is used at the SLC to measure A_b and A_c.

The τ-lepton polarization is measured both at LEP and SLC by, for example, the energy distribution of the π in $\tau^- \to \pi^- \nu_\tau$ decay. In the SM the τ-polarization, $P_\tau(\cos\theta)$, is dependent on both A_τ and A_e by

$$P_\tau(z) = -\frac{(1+z^2)(1+A_eP_e)A_\tau + 2(A_e+P_e)z}{(1+z^2)(1+A_eP_e) + 2(A_e+P_e)A_\tau z}, \qquad (10d)$$

where $z = \cos\theta$ and θ is the angle between the τ-lepton and the electron beam direction and P_e is the incident electron beam polarization ($P_e = 0$ at LEP). Both LEP and SLD have determined A_e and A_τ by this method. The SLD collaboration exploits the polarized incident electron beam[6] to measure an asymmetry enhanced by a large factor (~3.4 at large $|\cos\theta|$).

3 Lepton Asymmetries

Lepton asymmetries derived from pure leptonic final states $Z^0 \to l^+l^-$ are the easiest to interpret as precision tests of the SM. Nevertheless, the b-quark asymmetry, exploited by the LEP experiments, offers a high statistical precision method within the context of the SM for determining the electron asymmetry, A_e.

3.1 Pure Lepton Modes

The single most precise determination of the electron asymmetry and thus of $\sin^2\theta_w^{eff}$ comes from the measurement at the SLD of the total e^+e^- cross-section asymmetry A_{LR}, defined by Eq. 10b. The measurement directly determines A_e, the electron coupling asymmetry, with only small corrections and is only possible with incident polarized beams. Events for the A_{LR} analysis are selected to be "hadronic" and not a beam background, 2γ, or Bhabha event. Small experimental corrections of order $\leq 0.3\%$ are made for backgrounds, experimental asymmetries and direct channel γ exchange, and $Z^0\gamma$ interference. The systematic error of the measurement of A_{LR} is dominated by the electron beam polarization uncertainty. The electron beam polarization is directly measured by means of a Compton polarimeter[1] throughout data taking, with running averages updated at least as frequently as every hour, giving rise to an estimated systematic error presently at the level of $\Delta P_e/P_e \sim 0.7\%$ for the '94-'95 period and ~ 1.1% for '97-'98 data.

The lepton coupling asymmetry parameters A_L, for L = e, μ, and τ have been directly measured[7] using the corresponding *lepton final states* by the FB-LR asymmetry of Eq. 10c. The resulting cross sections are shown in Fig. 2. Although this test is of limited statistics (e, μ, τ: 9.4K, 7.6K, 7.1K events), is a direct measurement of A_μ and A_τ, a confirmation of A_e using the electron final state, and a probe of lepton universality. A maximum likelihood method is used to determine the coupling asymmetries which takes into account all known cross section terms (ten terms for the e^+e^- final state), backgrounds, and detection efficiencies.

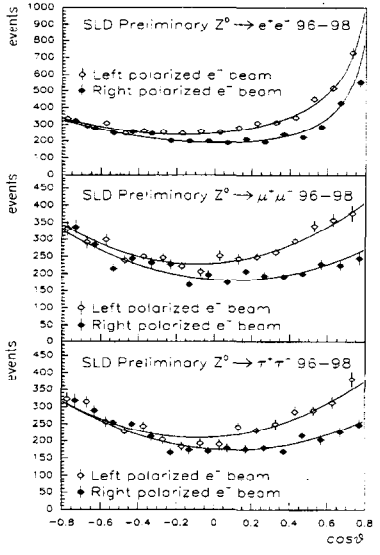

Figure 2: The differential cross sections measured at the SLD for $e^+e^- \rightarrow Z^0 \rightarrow e^+e^-$, $\mu^+\mu^-$, and $\tau^+\tau^-$ are shown.

At the end of the '97-'98 run, several important checks of the SLC parameters were performed which are important to certify the small corrections of γ exchange and γ–Z^0 interference and to make certain that the SLC positrons are not polarized. In order to check the energy calibration of the electron and positron spectrometers, which follow the beam interaction point, the Z^0 cross section peak was scanned and matched to the Z^0 mass determined at LEP-I. It was determined that the energy scale is known to about 40 MeV, which results in a negligible correction to $\sin^2\theta_w^{eff}$ (0.00011 ± 0.00009). In addition, a putative positron polarization was sought by directly measuring the positron beam polarization by means of a Møller polarimeter located in End Station A and found to be consistent with zero ($P_{e+} = -0.02 \pm 0.07\%$). Finally, the Compton polarimeter, which measures the electron polarization, was questioned but found to be in good agreement with measurements of the energy asymmetry of back-scattered Compton gammas detected by a threshold Cherenkov gas counter and a quartz fiber- tungsten radiator calorimeter.

In Table 3 we summarize the world's data on lepton coupling asymmetries[7,8] (both SLD[7] and LEP[8] data are preliminary).

Table 3: Lepton Coupling Asymmetries.

Quantity	Asymmetry
SLD: A_{LR}	0.1510 ± 0.0025
SLD: A_e	0.1504 ± 0.0072
SLD: A_μ	0.120 ± 0.019
SLD: A_τ	0.142 ± 0.019
SLD: $\langle A_{e,\mu,\tau} \rangle$	0.1459 ± 0.0063
SLD: A_{LR}, $\langle A_{e,\mu,\tau} \rangle$	0.1503 ± 0.0023
LEP: A_{FB} (l), $A_{e,\mu,\tau}$	0.1469 ± 0.0027
SLD+LEP	0.1489 ± 0.0018

We note that the LEP-I values and those from the SLC-SLD are in good agreement with the resulting value of leptonic asymmetries differing by only ~ 1 σ.

3.2 A_e from b-Quark Asymmetry

The experiments at LEP have exploited $Z^0 \to b\bar{b}$ data to determine A_{FB}^{0b}, the b-quark asymmetry at the pole, and hence A_e within the context of the SM (see Eq. 10a). The method rests on the assumption that A_b, the asymmetry parameter of the b-quark coupling, agrees with the SM prediction since what is actually measured in A_{FB}^{0b} is the product of A_b and A_e. Even within the context of the SM, important corrections are needed before an accurate value of A_e can be extracted from A_{FB}^{0b}. The c-quark background can dilute the b-asymmetry since this background enters with a smaller asymmetry and opposite electric charge. The jet charge method is especially sensitive to this correction. QCD effects, which tend to smear the direction of the final state quarks and make the measured asymmetry smaller, and $B-\bar{B}$ flavor mixing are two other corrections, which must be included. The resulting A_{FB}^{0b} measurement from LEP is 0.0991 ± 0.0021. Using the SM value of $A_b = 0.935$, the corresponding value of $A_e = 0.14145 \pm 0.0030$, which is 2.1 σ different from the pure lepton-based determinations above.[7]

4 Determination of $\sin^2\theta_w^{eff}$

The value of $\sin^2\theta_w^{eff}$ can be determined through Eqs. 3 and 5b, and the results are given in Table 4. The right-most column indicates the χ^2/DoF of the LEP measurements alone and of the LEP and SLC preliminary measurements combined. We take these data to be in generally good agreement, although we note that the pure leptonic-derived values of $\sin^2\theta_w^{eff}$ measured at the SLC and LEP are smaller than the value derived from A_{FB}^{0b} at LEP.

Table 4: Effective mixing angle at the Z^0 pole.

Measurement	$\sin^2\theta_w^{eff}$	χ^2/DoF
SLC:A_{LR},<A_e,μ,τ>	0.23110 ± 0.00029	
LEP: A_{FB}^{0l}	0.23117± 0.00054	
LEP: A_τ	0.23202 ± 0.00057	
LEP: A_e	0.23141± 0.00065	
LEP leptonic	0.2316 ± 0.0004	1.2/2
SLC+LEP leptonic	0.23127 ± 0.00023	
LEP: A_{FB}^{0b}	0.23223 ± 0.00038	
LEP: A_{FB}^{0c}	0.2320 ± 0.0010	
LEP: <Q_{FB}>	0.2321± 0.0010	
LEP average	0.23187 ± 0.00024	3.2/5
LEP+SLC average	0.23156 ± 0.00018	7.3/6 all

The χ^2/DoF of all data is 7.3/6 (~ 32 % CL), whereas for only lepton-based measurements χ^2/DoF = 3.7/3 (~ 35 % CL)—both in reasonable agreement. Later, we make an observation on the nature of the $\sin^2\theta_w^{eff}$ value derived from A_{FB}^{0b} at LEP and the experimental value of A_b.

5 Standard Model Tests with s, c, and b Quarks

It is interesting to see if the coupling constants g_V and g_A for the s, c, and b quarks follow the predictions of the SM. Two variables are accessible for this test of the SM: the coupling constant asymmetry and the branching ratio. The coupling constant asymmetry measures the combination $A_f = 2g_{Vf}/g_{Af}/(1+(g_{Vf}/g_{Af})^2)$ and the branching

ratio for Z^0 to decay into a quark favor, f, determines the combination $R_f = \Gamma_f / \Gamma_{had} \sim (g_{Vf}^2 + g_{Af}^2)$. To check theory, the vector and axial vector couplings are taken from the average value of $\sin^2\theta_w^{eff}$ derived from global fits, where the overall consistency of the data is checked. Or more strictly, the value of $\sin^2\theta_w^{eff}$ is taken from purely lepton measurements, thereby probing the universality of $\sin^2\theta_w^{eff}$ across lepton-quark families. In the case of the $Z^0 \to b\bar{b}$ vertex (also $Z^0 \to s\bar{s}$), since $g_L^2 \sim 30\ g_R^2$, R_b has a large sensitivity to the *left-handed* coupling, such as vertex corrections involving $W^{\pm}$, $t^{\pm}$ exchange, whereas A_b has a greater sensitivity to the *right-handed* components. We find the following sensitivities for $\sin^2\theta_w^{eff} \approx 0.23$

$$\frac{\delta R_b}{R_b} \sim -3.6\ \delta g_{Lb} + 0.7\ \delta g_{Rb}\ , \qquad (11a)$$

$$\frac{\delta A_b}{A_b} \sim -0.3\ \delta g_{Lb} + 1.7\ \delta g_{Rb}\ . \qquad (11b)$$

Thus, R_b and A_b are complementary measurements and probe different sectors of the theory.

The SLD brings a number of experimental tools to the study of the electroweak couplings of s, c, and b quarks. The pixel vertex detector can identify displaced vertices from the IP as a signature for b and c quark final states, and the Cherenkov Ring Imaging Detector (CRID) can identify $\pi^{\pm}$, $K^{\pm}$, $p^{\pm}$ particles in the final state. Various discriminants are used to isolate s-, c-, and b-quark events, which result for example in a hemisphere b-tag efficiency and purity in the range of 45% and 99%, respectively.

The most powerful test of the SM for quark final states have come from a study of the b-system. Several factors conspire to allow this.

(1) The asymmetry parameter A_b is expected to be only weakly dependent on $\sin^2\theta_w^{eff}$ (see the entry for d-quarks in Table 2), thus the measurement of A_{FB}^{0b}, given by Eq. 10a, is mostly a determination of A_e.

(2) The b-quark has a large branching ratio (~22%) and thus has a small statistical error for reasonable detection efficiency.

(3) b-quark events can be separated from other hadronic events by detection of displaced secondary vertices and various event attributes, such as high transverse mass.

(4) The b-quark charge can be determined by a variety of experimental signatures, such as a high P_t charged lepton, jet charge, kaon charge and, in the SLD, initial state tagging through the incident electron beam polarization.

(5) A_{FB} varies with center-of-mass energy, and when measured below and above the Z^0 peak at LEP, has a larger asymmetry, thereby adding information to the small asymmetry at the pole.

Similar arguments hold for s-quark and c-quark final states (no flavor mixing), although the c-quark final state is more sensitive to $\sin^2\theta_w$, thereby making the test of the SM more involved. Further, c-quarks are more difficult to separate from background and their detection frequently exploits "charm counting" where all charm hadrons which eventually decay via D^0, D^+, D_s, and Λ_c are summed, or by the reconstruction of D*s, yielding a clean sample of events. A lepton fit is also used to separate c (and b) events from background.

The coupling constant asymmetry measurements are not sensitive to the detection efficiency, although the background dilution in the asymmetry is. For the branching ratio analysis the detection efficiency critically enters and it is highly beneficial to achieve high detection efficiency since, for example, $\delta R_b \sim 1/\varepsilon_b$.

5.1 Measurements of A_S, A_C, and A_b

The SLD has measured A_s, A_c, and A_b directly through Eq. 10c, which depends critically on a precise knowledge of the electron beam polarization, P_e, but is a direct and powerful method largely independent of the Z^0-leptonic coupling physics.[9,10,11] Figure 3 shows the left and right asymmetries as determined by jet-charge for b-quarks as observed by the SLD.[11] (See Fig. 1 for the relevant physics at the tree-level.) LEP derives the asymmetry parameters from the forward-backward composite asymmetry, A_{FB}, given by Eq. 10a. For the extraction of A_b and A_c using A_{FB}, a value of A_e derived from other measurements must be used.

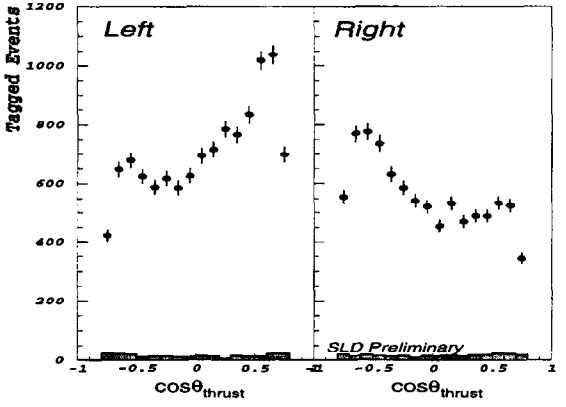

Figure 3: The θ-angle distribution for b-quarks produced from left and right electron beam polarizations at the SLD, indicating the forward-backward left-right asymmetry in b-quark production as measured by the jet-charge asymmetry.

The resulting asymmetries determined at LEP and SLC are given in Tables 5, 6, and 7 for A_s, A_c, and A_b, respectively. The LEP A_{FB} asymmetries have been corrected by the factor $4/(3\,A_e)$ with $A_e = 0.1491 \pm 0.0018$ (average of A_{LR} and LEP leptonic). In the tables the combined averages have taken into account correlations between measurements.

The SLD determination of A_S is derived from a sample of approximately 300K hadronic decays of Z^0 bosons produced with a polarized electron beam. The $s\bar{s}$ sample was selected by suppressing heavy quark decays (c and b) by requiring well-reconstructed tracks to have a transverse impact parameter with the IP of less than three times the estimated resolution. The impact parameter resolution obtained from our upgraded CCD vertex detector, VXD3, is given by $\sigma_d = 9 \oplus 29/(p_\perp \sin^{3/2}\theta)\,\mu m$, where θ is the polar angle of the track with respect to the beam. Further refinements of the $s\bar{s}$ sample were obtained by using the Cherenkov Ring Imaging Detector (CRID) to identify $K^\pm$. In addition, K^0_S and $\Lambda^0/\bar{\Lambda}^0$ were reconstructed and employed as tags of the $s\bar{s}$ final state.

Table 5: $A_{d,s}$ measurements from LEP and SLC (Summer 1998).

Experiment	Method	Asymmetry
SLD	A_S	$0.82 \pm 0.10 \pm 0.07$
DELPHI: (1995)	A_S	$1.165 \pm 0.311 \pm 0.116$
DELPHI: (1995)	$A_{d,s}$	$0.996 \pm 0.276 \pm 0.480$
OPAL: (1997)	$A_{d,s}$	$0.605 \pm 0.311 \pm 0.098$
LEP average		0.91 ± 0.21
LEP+SLD average		0.84 ± 0.10

Each of the two hemispheres, defined by the perpendicular plane bisecting the thrust axis, was required to have at least one identified strange particle. Overall, the purity of the $s\bar{s}$ final state was estimated to be 69% with 10% $u\bar{u}$, 9% $d\bar{d}$, 11% $c\bar{c}$, and 1% $b\bar{b}$ contamination. A binned maximum likelihood fit was performed to determine A_s. The procedure included particle detection efficiencies and acceptances.

Taking $\sin^2\theta_w^{eff} = 0.23155$, the SM predicts $A_S = 0.935$, a value which is slowly varying with $\sin^2\theta_w^{eff}$. The table indicates that the preliminary SLC value of A_S is 1.0 σ low with respect to the SM and the LEP value is 0.1 σ low (with A_e correction made). The SLD+LEP average is dominated by the SLC value and is 1.0 σ low.

The SLD brings excellent vertex detector and particle identification to the isolation of $c\bar{c}$ events. From the ensemble of hadronic events, secondary vertices possibly signifying $c\bar{c}$ events are identified by means of a topological algorithm,[12] which searches for space points in three dimensions where the reconstructed tracks overlap. Tracks, in this algorithm, are considered probability "tubes." The method finds secondary vertices in 84% of b, 38% of c, and 2% of light quark events under the requirement that the secondary vertex be displaced from the IP by at least 1 mm. Further refinement of the charm sample is obtained by reconstructing the mass of the tracks associated with the secondary vertex—a calculation aided by the well-defined IP of the SLC and our high resolution pixel vertex detector. The mass is defined as $M = \sqrt{M_{ch}^2 + P_t^2} + |P_t|$, where M_{ch}^2 is the mass of the ensemble of charged tracks associated with the secondary vertex and P_t is the net transverse momentum with respect to the line connecting the secondary vertex and the IP. Charm candidates were required to have a vertex mass in the range $0.55 < M_c < 2$ GeV/c^2. By vetoing on b-events and imposing momentum cuts, charm events are isolated with 81% purity. Several methods are employed to determine the direction of the charm quark needed for the $A_{FB\text{-}LR}$ evaluation, such as vertex charge, $K^{\pm}$ tag, lepton tag and D^*, D^+ identification. These tags have different efficiencies in the range of ~ 30%. A maximum likelihood fit to all tagged events is used to determine A_c.

Referring to Table 6, the A_c LEP-SLC average is in good agreement (only 0.6 σ) with the SM value of $A_c = 0.668$ for $\sin^2\theta_w^{eff} = 0.23155$ with the preliminary SLD value lower than the SM by about 0.5 σ and the LEP value low by 0.9 σ. The LEP values are derived from measurements which average to $\langle A_{FB}^{0,c} \rangle = 0.0714 \pm 0.0044$, which is then corrected by $4/(3\ A_e)$.

Table 6: A_c measurements from LEP and SLC (Summer 1998).

Experiment	Method	A_c
SLD	K & vtx-Q	$0.65 \pm 0.04 \pm 0.03$
SLD	lepton	$0.70 \pm 0.09 \pm 0.07$
SLD	D^*, D^+	$0.63 \pm 0.06 \pm 0.04$
SLD average		0.649 ± 0.040
DELPHI	lepton	$0.73 \pm 0.10 \pm 0.11$
L3	lepton	$0.82 \pm 0.29 \pm 0.19$
ALEPH	D^*	$0.63 \pm 0.08 \pm 0.02$
DELPHI	D^*	$0.64 \pm 0.08 \pm 0.04$
OPAL	D^*	$0.62 \pm 0.11 \pm 0.05$
LEP average		0.634 ± 0.040
LEP+SLD average		0.642 ± 0.028

A summary of measurements of A_b is shown in Table 7, where correlations were taken into account in the computation of averages. The SM predicts $A_b = 0.935$ for $\sin^2\theta_w^{eff} = 0.23155$, which is 3.2 σ larger than the world average for the measurement. We note that the LEP and preliminary SLC values are consistent; the SLC value is 1.9 σ lower than the SM, and LEP is 2.3 σ low.

Table 7: A_b measurements from LEP and SLC (Summer 1998).

Experiment	Method	A_b
SLD	jet charge	$0.849 \pm 0.026 \pm 0.031$
SLD	lepton	$0.932 \pm 0.058 \pm 0.038$
SLD	$K^{\pm}$ tag	$0.854 \pm 0.088 \pm 0.106$
SLD average		0.866 ± 0.036
ALEPH	lepton	$0.908 \pm 0.041 \pm 0.020$
DELPHI	lepton	$0.904 \pm 0.057 \pm 0.026$
L3	lepton	$0.869 \pm 0.055 \pm 0.030$
OPAL	lepton	$0.851 \pm 0.038 \pm 0.021$
ALEPH	jet charge	$0.953 \pm 0.037 \pm 0.029$
DELPHI	jet charge	$0.898 \pm 0.042 \pm 0.021$
L3	jet charge	$0.806 \pm 0.106 \pm 0.051$
OPAL	jet charge	$0.898 \pm 0.047 \pm 0.037$
LEP average		0.885 ± 0.022
LEP+SLD average		0.880 ± 0.017

The analysis of A_b involves many of the same considerations as discussed above for the extraction of A_c. A vertex mass tag is used, as in the case of A_c, but for the $b\bar{b}$ events it becomes more effective because the b-quark is heavier than any other visible quark, and hence has a large vertex mass which can be well separated from background. By requiring $M_b > 2$ GeV/c^2, the b-quark purity is 97% with an efficiency of 76%. Several strategies are used to determine the direction of the b-quark, such as jet charge, lepton tag, or a $K^{\pm}$ tag, which exploits the $b \rightarrow c \rightarrow s$ decay cascade. All methods have to rely on Monte Carlo simulations to a greater or lesser extent. The jet charge method has the advantage in that it is self-calibrating. Again, the LEP values for A_b are derived from measurements of A_{FB}^{0b}, which have an average value of $\langle A_{FB}^{0b} \rangle = 0.0991 \pm 0.0021$, and are corrected by the factor $4/(3A_e)$.

5.2 Measurements of R_c and R_b

The Z^0 branching fractions R_c and R_b are interesting places to search for violations of the SM. The largest known radiative corrections to R_b in the SM are charged-current vertex diagrams, which are dominated by the top quark.[13] In the past, R_b has stirred considerable interest in that the measurements were in significant disagreement with the SM. In the summer of 1995, for example, the value of R_b was almost four standard deviations different from the SM. However, a new analysis presented at ICHEP '96 by ALEPH,[14] which, among several improvements, reduced hemisphere correlations by reconstructing the primary vertex in each hemisphere for each event, resulted in a precise value of R_b in close agreement with the SM.

Tables 8 and 9 summarize the R_c and R_b measurements, respectively, from LEP[8] and SLC.[15,16] A double tag method is used in both the R_c and R_b analyses, where the heavy quark tagging procedure outlined above is applied independently to each thrust hemisphere of all hadronic events. Determining the single tag, double tag, and mixed tag rates, enables the tagging probability to be estimated by the data itself. A set of equations is developed in which either R_c and R_b can be determined, which avoids

large uncertainties of a direct calculation of the single tag efficiency. The b-tagging efficiency is typically $\varepsilon_b \sim 35\%$ with a hemisphere correlation of $\lambda_b \sim 0.6\%$.

The R_c world average is within 0.2 σ of the SM value of $R_c = 0.1723$. The SLC values are considered preliminary. The R_b world average of Table 9 is within 1.4 σ of the SM value of $R_b = 0.2155$. Hence the interesting 4 σ discrepancy with the SM of the summer 1995 has dissolved into fairly good agreement.

Table 8: Measurements of R_c (Winter 1998).

Experiment	Method	R_c
SLD	VTX-mass	0.1794 ± 0.0085 ± 0.0061
ALEPH	lepton	0.168 ± 0.006 ± 0.010
DELPHI	lepton	0.164 ± 0.009 ± 0.020
ALEPH	c-counting	0.176 ± 0.005 ± 0.011
DELPHI	c-counting	0.168 ± 0.011 ± 0.013
OPAL	c-counting	0.167 ± 0.011 ± 0.011
ALEPH	D* incl/excl	0.166 ± 0.012 ± 0.009
DELPHI	D* incl/excl	0.176 ± 0.015 ± 0.015
OPAL	D* incl/excl	0.180 ± 0.011 ± 0.013
ALEPH	D* excl/excl	0.173 ± 0.014 ± 0.009
DELPHI	D* incl/incl	0.171 ± 0.013 ± 0.015
SLD+LEP average		0.1731 ± 0.0044

Table 9: Measurements of R_b (Summer 1998).

Experiment	Method	R_b
SLD (prelim.)	VTX+mass	0.2159 ± 0.0014 ± 0.0014
ALEPH	multi-var	0.2159 ± 0.0009 ± 0.0011
DELPHI	multi-var	0.2163 ± 0.0007 ± 0.0006
L3	impact+lept	0.2176 ± 0.0015 ± 0.0026
OPAL	VTX+lept	0.2176 ± 0.0011 ± 0.0014
LEP+SLD average		0.21656 ± 0.00074

5.3 Comment on A_b and $\sin^2\theta_w^{eff}$

A_b itself shows the same difference as we observed in the $\sin^2\theta_w^{eff}$ value derived from $A_{FB}^{0,b}$ above—namely $A_{FB}^{0,b}$ measured is smaller than the prediction of the SM, resulting in a larger value of $\sin^2\theta_w^{eff}$ from the LEP measurements. Remember that we have used the pure leptonic determination of A_e to correct the LEP forward-backward asymmetries in order to obtain the value of A_b by the factor $4/(3A_e)$. Also note that the SLD measures A_b directly by means of the forward-backward left-right asymmetry.

Examining the factors involved, we conclude that the discrepancy in $\sin^2\theta_w^{eff}$ between LEP and the SLD is consistent with a discrepancy of the value of A_b from the SM. In fact, if we take the direct measurement of A_b from the SLD to derive the

value of A_e from the LEP value of $A_{FB}^{0,b}$ we obtain a value of $\sin^2\theta_w^{eff}$ which is *consistent with the pure leptonic value*. The equation below shows this calculation.

$$A_e = \frac{4}{3}\frac{A_{FB}^{0,b}(LEP)}{A_b(SLD)} = \frac{4}{3}\frac{0.0991\pm0.0021}{0.866\pm0.036} = 0.1526\pm0.0071 \qquad (12)$$

which results in $\sin^2\theta_w^{eff} = 0.2308 \pm 0.0009$—in good agreement (0.5 σ) with the pure leptonic value of $\sin^2\theta_w^{eff} = 0.23127 \pm 0.00023$. If the value $A_b(LEP) = 0.885 \pm 0.022$ (completely correlated with $A_{FB}^{0,b}$) is used instead, then $\sin^2\theta_w^{eff} = 0.23112 \pm 0.00038$ is obtained.

In a more sophisticated context, the analysis of Takeuchi, Grant, and Rosner[17] shows that the data of LEP and SLD are consistent in the pure leptonic sector and that the (current) major discrepancy (3.2 σ too low) is in the value of A_b. The left-handed coupling of the b-quark is tightly constrained by R_b and is in agreement with the SM. A_b is sensitive primarily to the right-handed coupling and is not in agreement with the SM (see Eqs. 11a and 11b). Figure 4 shows the analysis of the current experimental situation.

The TGR[17] variable ζ_b is sensitive to the parity violation of the b-quark, as measured by A_b. Its value is insensitive to the value of $\sin^2\theta_w^{eff}$—hence the horizontal band in Fig. 4. A_{LR} from SLC and A_e from LEP are most strongly dependent on $\sin^2\theta_w^{eff}$—hence the vertical bands.

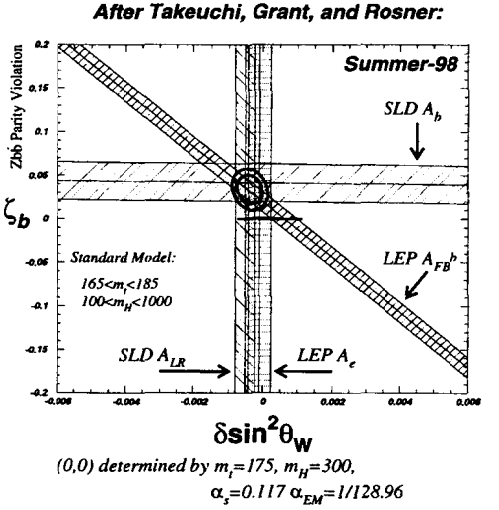

Figure 4: The consistency of the world's data is shown by the overlap of the measurement bands. The inconsistency with the SM is indicated by the offset of the overlap of measurements with the expectation of the SM given by the (0,0) point of the figure.

6 Radiative Corrections

We have observed that the data of LEP and SLD generally agree with the predictions of the Standard Model, although there is some concern over the discrepancy of A_b, and consequently the value of $\sin^2\theta_w^{eff}$ derived from the b-quark sector. So far, we have checked that Eq. 3 is generally valid, namely that the vector and axial vector couplings of a fermion to the Z^0 boson follow the weak isospin assignments and depend on the electric charge and effective weak mixing angle in a universal way. This is a test of the $SU(2)_L$ X U(1) gauge structure of the theory.

In order to check the theory beyond the "tree level" radiative corrections must be included. This process is usually performed by fitting all the measured quantities at the Z^0 pole with radiative corrections to derive the top quark mass and the Higgs mass, or constraining the top quark mass by the measured value at FNAL and deriving the Higgs mass. The consistency of the theory is measured by the quality of the fit. Sensitivities to M_t and M_h arise from different measured quantities having different dependencies on the parameters of the radiative corrections. We have already absorbed the vertex corrections for leptons (but not for quarks) by defining an effective mixing angle determined by A_e, the electron coupling constant asymmetry.

There have been a number of theoretical treatments which make the comparison of theory to data less model-dependent.[18] Here we adopt a more pedestrian approach and use "experimental" parameters, such as M_t and M_h to obtain an estimate of the magnitude of various terms. The need for radiative corrections is easily demonstrated in a naive evaluation of Eq. 2 using the value of $\sin^2\theta_w^{eff}$ determined above, α_{em} given by atomic physics experiments, and G_F from muon decay. This naive exercise predicts M_Z = 88.38 ± 0.03 GeV and M_W = 77.48 ± 0.04 GeV, values which are embarrassingly discrepant with the measured values of 91.1867 ± 0.0021 GeV and 80.37 ± 0.090 GeV, respectively [Vancouver 1998].[8]

Radiative corrections are grouped into two general types: (1) electromagnetic corrections, which include initial and final state radiation, vertex diagrams, etc., and the running of α_{em} for the atomic energy scale $q^2 \approx 0$ to the $q^2 = M_Z^2$; and (2) electroweak corrections where some of the corrections are absorbed in the definition of $\sin^2\theta_w^{eff}$, isospin-breaking loop terms in W and Z propagators, running of the Z self-energy, corrections to the $Z \rightarrow b\bar{b}$ vertex, and corrections to the W mass.

7.1 Hadronic Vacuum Polarization

Much of the discrepancy in the vector boson mass relations is corrected by the running of $\alpha_{em}(Q^2)$. The QED coupling at the M_Z scale is related to its value at low energy, given precisely in atomic physics experiments by

$$\alpha_{em}(M_Z^2) = \frac{\alpha_{em}(0)}{1 - \Delta\alpha_{em}(M_Z^2)}, \qquad (13)$$

where $\Delta\alpha_{em}(M_Z^2) = -\Pi_{\gamma\gamma}$ is the photon self-energy. The photon self-energy is evaluated quite accurately for leptons, but not for quarks. In order to evaluate the quark contribution, the measured e^+e^- hadronic cross section is employed to determine the value of a dispersion integral. Ironically, the data in the 1.05 to 5 GeV region, well beneath the scale of the Z^0 pole, contribute a large fraction of the integral as well as a large part of the uncertainty. Much of the data in this energy region are old and have large normalization errors. Further, above the charm threshold, many channels with different properties exist, complicating the evaluation of the integral. A number of evaluations have been performed.[19] The result adopted by the LEP EW-WG is $\alpha_{em}(M_Z^2) = 1/(128.896 \pm 0.090)$, which is an evolution of $\Delta\alpha/\alpha \sim 0.063$. In this formulation G_F does not run.[20]

7.2 Electroweak Radiative Corrections

The radiative corrections are furnished by the terms ζ in Eqs. 2 and 5 above. At the one-loop level the correction terms for the M_Z mass relation given by Eq. 2a is

$$\zeta_Z = (1 + \Delta\rho)\,(1 + \Delta_{3Q}), \tag{14a}$$

where, for leading order with M_t = 175 GeV and M_h = 160 GeV, the isospin-breaking loop corrections to the $W^{\pm}$ and Z propagators and Z self-energy terms, respectively, are

$$\Delta\rho \approx \frac{\alpha}{\pi}\frac{M_t^2}{M_z^2} - \frac{\alpha}{4\pi}\ln\frac{M_h^2}{M_z^2} \sim 0.0084 \quad , \tag{14b}$$

and

$$\Delta_{3Q} \approx \frac{\alpha}{9\pi}\ln\frac{M_h^2}{M_z^2} \sim 0.00031. \tag{14c}$$

The overall electroweak correction to the Z-mass relation is dominated by the quadratic M_t term and has the magnitude, $\Delta\zeta_z/\zeta_z \sim 0.0087$. The corresponding correction for M_W (Eq. 2b) is

$$\zeta_W = 1 - \Delta r_{ew}. \tag{15a}$$

where

$$\Delta r_{ew} \approx -\frac{c_0^2}{s_0^2}\Delta\rho \sim -0.028 \tag{15b}$$

with $s_0^2 c_0^2 = \pi\,\alpha_{em}(M_z^2)/\sqrt{2}\,G_F M_z^2$, yielding $\Delta\zeta_W/\zeta_W \sim 0.028$. The correction to the $Z^0 \rightarrow b\bar{b}$ partial width is given by

$$\zeta_{b\bar{b}} = (1+\delta_{QCD})\,(1+\delta_{vb}). \tag{16a}$$

The QCD component to next-to-leading order is

$$\delta_{QCD} \approx \frac{\alpha_s(M_z^2)}{\pi} + 1.41\left(\frac{\alpha_s(M_z^2)}{\pi}\right)^2 \sim 0.038 \tag{16b}$$

for $\alpha_s(M_Z^2) = 0.12$. The vertex correction, δ_{vb}, is

$$\delta_{vb} \approx -\frac{20}{13}\frac{\alpha}{\pi}\left(\frac{M_t^2}{M_z^2} + \frac{13}{6}\ln\frac{M_t^2}{M_z^2}\right) \sim -0.025. \tag{16c}$$

In addition to the QCD and vertex corrections for Γ_{bb}, there are QED and finite mass terms. From the list above, the largest correction to the mass relations of Eqs. 2a and 2b is the running of α_{em} from the atomic scale to the M_z scale. Other corrections are quadratic in M_t, and logarithmic in M_h. Two-loop electroweak top corrections are being reconsidered[21] and may be important.

8 Global Test of the Standard Model

Within the context of the SM different electroweak observables are sensitive to different radiative correction parameters (M_t, M_h, α_s). For example, R_b has a strong sensitivity to M_t and little to M_h, M_W is sensitive to both M_t and M_h, and σ_{had}^0 depends on α_s. These different sensitivities are exploited to determine the value of M_t and set limits on M_h or with a constrained value of M_t determine (still within large errors) the value of M_h. Table 10 shows the results of a fit (ZFITTER 5.10)[22] to all the world's electroweak data [M_W, R_V, Γ_Z, σ_{had}^0, R_l, A_{FB}^l, A_e, A_t, A_{LR}, A_{FB}^b, A_{FB}^c, R_b, R_c, Q_{FB}, Q_W(Cs), and Q_W (Tl)].

Table 10: Results of a fit to electroweak data at Z^0 pole.

Parameter	Constraint	Best Fit
M_Z (GeV)	91.187±0.002	91.187
$1/\alpha_{em}(M_Z^2)$	128.928±0.023	128.928±0.023
M_t (GeV)	173.8 ± 5.0	172.2±4.8
$\alpha_s(M_Z^2)$	----------	0.119±0.003
$\log_{10}(M_h)$	----------	$1.981^{+0.216}_{-0.242}$
M_h (GeV)	----------	$95.6^{+61.6}_{-40.9}$
χ^2/DoF	----------	15.2/14 (37%)

The fitted value of M_t is in agreement with the direct observation at FNAL[23] of M_t = 173.8 ± 5.0 GeV. The limits on M_h are > 90 GeV from direct searches and < 280 GeV at 95% CL.[24]

It is interesting to note that the SLD value of $\sin^2\theta_w^{eff}$ implies a Minimal Standard Model (MSM) Higgs scalar of ~ 40 GeV and is ~ 1 σ in contradiction with the present direct search limit of > 90 GeV at the 95% CL, whereas the LEP value is consistent with M_h ~ 220 GeV and is not excluded by direct searches.

A more sophisticated way of looking at the data is shown in Figure 5 as a comparison of the world's data with the variables S and T of Peskin and Takeuchi.[25] The variables S and T are normalized to (0,0) at a nominal SM point—determined by the measured value of M_t and a nominal value of M_h. The contributions to isospin-violating mass differences beyond the set point are described by T, which is roughly quadratic in M_t and logarithmic in M_h (see Eqs. 14 and 15 above). The parameter S is sensitive to isospin-independent terms which would grow systematically with the size of a new sector. The Peskin-Takeuchi variable U is assumed to be 0 in this application. The 68% confidence region of the LEP and SLD data is indicated by the oval region in the figure.

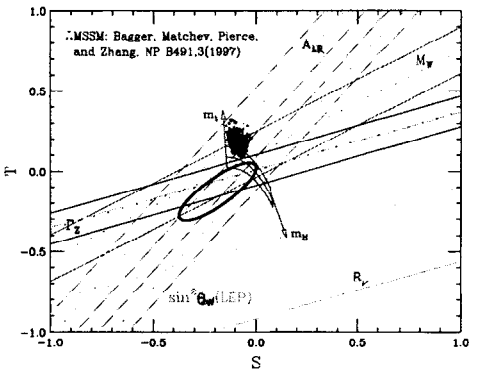

Figure 5: The S and T constraints provided by LEP, SLD, and FNAL are indicated. The SLD measurement of A_{LR} seems to prefer the MSSM of Pierce *et al.*[26]

The S-T region predicted by the MSM is indicated by the banana-region centered about the (0,0) point of the figure. In that region, the right-hand edge corresponds to M_h = 88 GeV and M_t = 173.9 ± 5.2 GeV. Increasing the Higgs mass up to 1 TeV is displayed by the width of the region. An indication of supersymmetry would be a shift of the experimental overlap region from the expectations of the MSM with S becoming slightly negative and T positive. The MSSM of Pierce *et al.*[26] is indicated by the ensemble of dots in the figure—each representing a choice of the five parameters of the model. We note the SLD data[27] favors a supersymmetric world, whereas LEP data disfavors the model by about 2 σ.

9 Summary and Conclusions

The Standard Model works remarkably well with only one parameter, A_b, out of some 18 measurements differing significantly from theory prediction.[28] The $SU(2)_L$ X U(1) structure of the theory is quite well established through one-loop electroweak radiative corrections, although the b-quark sector continues to exhibit troublesome inconsistencies. The largest discrepancies are $\Delta \sin^2\theta_w^{eff}$ (SLD versus LEP) ~ 2.2 σ and ΔA_b (SLD+LEP versus SM) ~ 3.2 σ. Most of the $\Delta \sin^2\theta_w^{eff}$ (SLD versus LEP) is resolved by considering only purely leptonic determinations of the electroweak mixing angle, isolating the puzzle of why A_b does not agree with the SM. Analyses of A_b are involved and, to a greater or lesser extent, rely on Monte Carlo simulation to estimate the experimental resolution, efficiency, and background. These simulations may be flawed in a subtle way and therefore contribute to the discrepancy—or there may be "new" physics at long last becoming visible in the b-sector. If the purely leptonic value (SLD and LEP) of $\sin^2\theta_w^{eff}$ is ultimately preferred, then the precision electroweak data suggest that the Higgs scalar is light and direct searches for it become quite tantalizing.

The SLD has proposed to take more data at the Z^0 pole, which will continue to probe the SM, especially in refining the measurement of $\sin^2\theta_w^{eff}$ and b-quark parameters. Data from LEP-II will decrease the uncertainty in M_W, explore the triple vertex coupling, and search for exotic particles beyond the SM. Tevatron at FNAL will decrease the M_t and M_W errors. And "modern" low energy data (Novosibirsk, BES, DAPHNE, B-factories) should improve the evaluation of $\Delta\alpha_{em}(M_Z^2)$ and sharpen the radiative corrections.

Acknowledgments

I would like to thank the organizers and participants of this conference for a very stimulating time. Special thanks go to my SLD colleagues and to the SLC Accelerator Department for their outstanding performance.

References

[1] M. Breidenbach, SLAC-PUB-3798 (1985); K. Abe *et al.*, Phys. Rev. D **53** (1996) 1023; M. Woods, SLAC PUB-7320 (1996) [hep-ex/9611006]; E. Torrence, SLAC-REPORT-509 (1997); A. Lath, SLAC-REPORT-454 (1994).

[2] K. Abe *et al.*, Nucl. Instrum. and Meth., A **400**, (1997), 287-343.

[3] S. Weinberg, Phys. Rev. Lett. **19** (1967) 1264; A. Salam, *Elementary Particle Theory*, edited by N. Svartholm, p. 367.

[4] See for example: D. C. Kennedy and B. W. Lynn, Nucl. Phys. B **322** (1989), 1.

[5] K. Abe *et al.*, Phys. Rev. Lett. **78** (1997) 2075-2079.

[6] K. Abe *et al.*, Phys. Rev. Lett. **79**, 804-808 (1997); R. S. Panvini, SLAC-PUB-7375; A. K. McKemey, in *Proceedings of ICHEP'96 Conference.*

[7] K. Abe et al., SLAC-PUB-7878 (1998).

[8] For recent LEP data see M. Martinez, *Precision Electroweak Results at LEP I and LEP II,* in these proceedings; see also D. Abbaneo *et al.*, ElectroWeak Working Group, Internal Memo LEPEWWG/97-01; CERN-PPE/97-154; J. Timmermans, in *Proceedings of XVIII Int. Sym. on Lepton-Photon Int.*, Hamburg (1997).

[9] SLD A_S: K. Abe *et al.*, SLAC-PUB-7825 (1998).

[10] SLD A_C: K. Abe *et al.*, SLAC-PUB-7879 (1998).

[11] A_b analyses from the SLD are discussed in K. Abe *et al.*, SLAC-PUB-7886 (1998); K. Abe *et al.*, SLAC-PUB-7959 (1998); see also Dong Su, in Heavy

Quark Couplings to the Z^0, presented at the *XVIII International Symposium on Lepton Photon Interactions* (1997), Hamburg, Germany.

[12] D. Jackson, Nucl. Instrum. and Meth., A **338**, (1997) 247.

[13] See for example: A. Blondel and C. Verzegnassi, Phys. Lett. B **311** (1993) 346–356.

[14] ALEPH: I. R. Tomalin, in *Proceeding of ICHEP'96*, Warsaw, Poland, p. 1340 (1996).

[15] SLD R_c: K. Abe *et al.*, SLAC-PUB-7880 (1998).

[16] SLD R_b: K. Abe *et al.*, Phys. Rev. Lett. 80 (1997) 660.

[17] T. Takeuchi, A. Grant and J. Rosner, p. 1231 in *Proceedings of 8th Meeting of the DPF* (Albuquerque, N.M. 1994), edited by S. Seidel.

[18] G. Altarelli, R. Barbieri, and S. Jadach, Nucl. Phys. B **369**, 3 (1992); W. Marciano, these proceedings.

[19] M. Swartz, Phys. Rev. D **53** (1996) 5268; H. Burkhardt and B. Pietrzyk , Phys. Lett. B **356** (1995) 398.

[20] R. D. Peccei, DESY 89-060.

[21] G. Degrassi et al., hep-ph/9412380.

[22] The fit uses ZFITTER, D. Bardin *et al.*, CERN-TH 6443/92 (May 1992); hep-ph/9412201.

[23] See R. Brock, in *Proceedings of Fund. Particles and Interactions,* p. 189, Nashville, TN, edited by R. S. Panvini and T. J. Weiler (1997); J. Kotcher, in these proceedings.

[24] D. Karlen, in *Proceedings of the 1998 Int. Conf. on High Energy Physics,* ICHEP'98, Vancouver, BC (1998).

[25] M. Peskin and T. Takeuchi , Phys. Rev. D **46**, 381-409 (1992).

[26] D. Pierce *et al.*, Nucl. Phys. B **491** (1997) 3-67.

[27] "Request for SLD Run Extension," SLD Collaboration (Aug. 1998).

[28] An earlier comparison of LEP-SLC data can be found in F. E. Taylor, in *Proceedings of Fund. Particles and Interactions*, p. 166, Nashville, TN, edited by R. S. Panvini and T. J. Weiler (1997).